Inorganic Chemistry

Article

pubs.acs.org/IC

Equilibrium and NMR Relaxometric Studies on the *s*-Triazine-Based Heptadentate Ligand PTDITA Showing High Selectivity for Gd^{3+} Ions

Zsolt Baranyai,*[,‡] Lorenzo Tei,[§] Giovanni B. Giovenzana,[⊥] Ferenc K. Kálmán,[‡] and Mauro Botta*[,§]

[‡]Department of Inorganic and Analytical Chemistry, University of Debrecen, H-4010, Debrecen, Egyetem tér 1, Hungary

[§]Dipartimento di Scienze e Innovazione Tecnologica, Università del Piemonte Orientale "Amedeo Avogadro", Viale T. Michel 11, I-15121 Alessandria, Italy

[⊥]Dipartimento di Scienze del Farmaco, Università degli Studi del Piemonte Orientale "Amedeo Avogadro", Largo Donegani 2/3, I-28100 Novara, Italy

Supporting Information

ABSTRACT: A complete potentiometric and NMR relaxometric solution study on the heptadentate 2,2′,2″,2‴-[(6-piperidinyl-1,3,5-triazine-2,4-diyl)dihydrazin-2-yl-1-ylidene]tetraacetic acid (PTDITA) ligand has been carried out. This ligand is based on the 1,3,5-triazine ring with two hydrazine-*N*,*N*-diacetate groups in positions 2 and 4 and a piperidine moiety in position 6. The introduction of the triazine ring into the ligand backbone is expected to modify its flexibility and then to affect the stability of the corresponding complexes with transition-metal and lanthanide ions. Thermodynamic stabilities have been determined by pH potentiometry, UV spectrophotometry, and ^{1}H NMR spectroscopy for formation of the complexes with Mg^{2+}, Ca^{2+}, Cu^{2+}, Zn^{2+}, La^{3+}, Gd^{3+}, and Lu^{3+} ions. PTDITA shows a good binding affinity for Gd^{3+} ($\log K$ = 18.49, pGd = 18.6) and an optimal selectivity for Gd^{3+} over the endogenous Ca^{2+}, Zn^{2+}, and Cu^{2+} ($K_{sel} = 6.78 \times 10^7$), which is 3 orders of magnitude higher that that reported for Gd(DTPA) ($K_{sel} = 2.85 \times 10^4$). This is mainly due to the lower stability of the Cu^{II}- and Zn^{II}(PTDITA) complexes compared to the corresponding DTPA complexes, which suggests an important role of the triazine ring on the selectivity for the Gd^{3+} ion. The relaxometric properties of Gd(PTDITA) have been investigated in aqueous solution by measuring the ^{1}H relaxivity as a function of the pH, temperature, and magnetic field strength (nuclear magnetic relaxation dispersion profile). Variable-temperature ^{17}O NMR data have provided direct information on the kinetic parameters for exchange of the coordinated water molecules. A simultaneous fit of the data suggests that the high relaxivity value (r_1 = 10.2 mM^{-1} s^{-1}) is a result of the presence of two inner-sphere water molecules along with the occurrence of relatively slow rotation and electronic relaxation. The water residence lifetime, $^{298}\tau_M$ = 299 ns, is quite comparable to that of clinically approved magnetic resonance imaging contrast agents. The displacement of the inner-sphere water molecules by bidentate endogeneous anions (citrate, phosphate, and carbonate) has also been evaluated by ^{1}H relaxometry. In general, the binding interaction is markedly weak, and only in the case of citrate, a ca. 35% decrease in relaxivity was observed in the presence of 60 equiv of the anion. Phosphate and carbonate also interact with the paramagnetic ion, likely as monodentate ligands, but formation of the ternary complex is accompanied by a modest increase of r_1 due to the contribution of second-sphere water molecules.

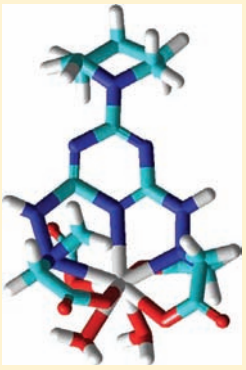

INTRODUCTION

The extensive use of lanthanide complexes for important applications such as diagnostic imaging, radiotherapy, luminescent probes, and other optical devices has prompted research into the development of structurally novel hexa-, hepta-, and octadentate polyaminopolycarboxylate ligands that are able to selectively coordinate a given trivalent cation of the lanthanide series.[1] Their physicochemical and structural properties are often investigated in great detail in order to get the information needed to improve their characteristics.

Among these, the use of paramagnetic gadolinium chelates as medical magnetic resonance imaging (MRI) contrast agents (CAs) was introduced in order to enhance the differences between normal and diseased tissue by markedly accelerating the $1/T_1$ relaxation rates of the hydrogen atoms of the body fluids.[2,3] Because of the importance of MRI in modern diagnostic medicine, the search for optimal CAs has increased considerably during the last 2 decades. According to the established theory of paramagnetic relaxation, the number (q) and residence lifetime, τ_M, of the metal-coordinated water (H_2O) molecule(s) and the rotational motion of the paramagnetic system, described by the correlation time τ_R, are the key parameters to be optimized.[2,3] Because of CA sensitivity limitations of MRI and the development of ever higher magnetic field strength MRI scanners, the synthesis of ligands capable of forming stable gadolinium(III) complexes with two (or more) H_2O molecules bound in the first (inner) coordination sphere (q = 2) has been pursued for a long time.[4] The difficult task is to increase the hydration state of the metal ion by reducing the number of donor atoms of the chelator without compromising the thermodynamic and kinetic

Received: November 28, 2011
Published: February 7, 2012

   dx.doi.org/10.1021/ic202559h | Inorg. Chem. 2012, 51, 2597−2607

stability of the complex. It is therefore important to study in detail the solution thermodynamic and kinetic behavior of the lanthanide(III) complexes with the novel ligands in order to ascertain their possible use in clinics or only in preclinical studies.[2,3] Both acyclic and macrocyclic polyaminocarboxylate ligands have been considered and investigated for the formation of q = 2 gadolinium(III) complexes.[4−6] Among these complexes, those formed with acyclic[7] and cyclic[8] pyridine-containing ligands have been extensively studied, for example, as luminescent probes for highly sensitive bioaffinity assay or as bimodal MRI and luminescent probes, providing simultaneously high MRI efficiency for the gadolinium(III) complex and remarkable optical properties for near-IR-emitting lanthanides.

We have recently reported the synthesis and ^{1}H and ^{17}O NMR relaxometric characterization of gadolinium(III) complexes with novel *s*-triazine (=1,3,5-triazine)-based polyaminopolycarboxylate heptadentate ligands.[9] In that case, it was unexpectedly found that the gadolinium(III) complexes are octacoordinate, possessing a single H_2O molecule in their inner coordination sphere. The exchange rate of the coordinated H_2O molecule was measured to be remarkably low, an unusual property for Gd^{III} chelates characterized by an octacoordinate ground state. More recently, the synthesis of the novel triazine-based ligand, shown in Scheme 1, H_4PTDITA = 2,2′,2″,2‴-[(6-piperidin-1,3,5-triazine-2,4-diyl)dihydrazin-2-yl-1-ylidene]-tetraacetic acid, has been reported together with a photophysical characterization of its europium(III) complex.[10]

Scheme 1. Chemical Structures of H_4PTDITA and H_4PyMTA[a]

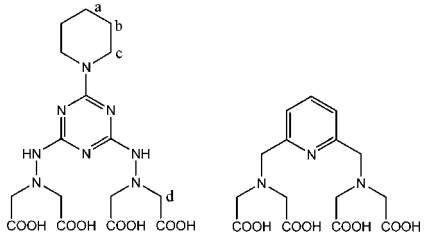

H_4PTDITA H_4PyMTA

[a] H_4PTDITA is presented with the labeling used to assign the NMR resonances.

H_4PTDITA can be regarded as a functionalized derivative of 1,3,5-triazine-2,4,6-triamine possessing two pendant iminodiacetate (IDA) moieties bound to the amino groups in positions 2 and 4 and a piperidine ring in position 6. By complex formation, the three nitrogen donors (two nitrogen atoms of the IDA moieties and one of the heterocycle) and the four carboxylate oxygen atoms should encapsulate the metal ion. In this work, we report the protonation constants and the thermodynamic stability constants of the complexes of H_4PTDITA with Mg^{2+}, Ca^{2+}, Cu^{2+}, Zn^{2+}, La^{3+}, Gd^{3+}, and Lu^{3+} as determined by pH potentiometry, UV spectrophotometry, and ^{1}H NMR spectroscopy. A detailed characterization of the $[Gd(PTDITA)(H_2O)_2]^{-}$ complex was performed in aqueous solution by relaxometric techniques by investigating the ^{1}H relaxivity dependence on the pH, temperature, and magnetic field strength. Information on the water exchange dynamics was also obtained from temperature-dependent ^{17}O NMR data.

EXPERIMENTAL SECTION

Equilibrium Measurements. The chemicals used for the experiments were of the highest analytical grade. The stock solutions of the different metal ions were prepared from the solid metal chlorides (Aldrich, 99.9%). The concentrations of the $MgCl_2$, $CaCl_2$, $ZnCl_2$, $CuCl_2$, and $LnCl_3$ solutions were determined by complexometric titration with standardized Na_2H_2EDTA and Xylenol Orange ($ZnCl_2$, $LnCl_3$), murexide ($CuCl_2$), Patton & Reeder ($CaCl_2$), and Eriochrome Black T ($MgCl_2$) as indicators. The concentration of H_4PTDITA was determined by pH-potentiometric titration in the presence and absence of a large (40-fold) excess of $CaCl_2$. PTDITA was prepared as previously reported.[10]

The protonation and stability constants of some metal complexes formed with the PTDITA ligand were determined by pH-potentiometric titration. The metal-to-ligand concentration ratios were 1:1, but for the copper(II) and zinc(II) complexes, titrations were also made at a metal-to-ligand ratio of 2:1 (the concentration of the ligand was generally 0.002 M).

For the pH measurements and titration, a Radiometer PHM93 pH meter, an ABU 80 autoburet, and a Metrohm-6.0234.100 combined electrode were used. Equilibrium measurements have been carried out at a constant ionic strength (0.1 M, KCl) in 10 mL samples at 25 °C. The solutions were stirred, and N_2 was bubbled through them. The titrations were made in the pH range 1.7−11.7. For calibration of the pH meter, potassium hydrogen phthalate (pH = 4.005) and borax (pH = 9.177) buffers were used. For calculation of $[H^+]$ from the measured pH values, the method proposed by Irving et al. was used.[11] A 0.01 M HCl solution was titrated with the standardized KOH solution. The differences between the measured and calculated pH values were used to obtain the H^+ concentration from the pH values, measured in the titration experiments.

The stability constant of Cu(PTDITA) has been determined by studying the equilibrium in the Cu^{2+}/PTDITA/ethylene glycol bis(2-aminoethyl ether)-*N*,*N*,*N*′,*N*′-tetraacetic acid (EGTA) system with UV−vis spectrophotometry. Spectrophotometric measurement were carried out on the absorption band of Cu(PTDITA) and Cu(EGTA) in the wavelength range 400−800 nm. Three series of samples were prepared, containing [EGTA] = 5.1×10^{-4}, 2.25×10^{-3}, or 5.03×10^{-3} M, [PTDITA] = 1.47×10^{-3} M, $[Cu^{2+}] = 1.47 \times 10^{-3}$ M, and [KCl] = 0.1 M. In each series, three samples (3 × 5 mL) were prepared with the different pH values in the pH range 7−7.5. The samples were kept at 25 °C for about 2 weeks in order for equilibrium to be attained (the time needed to reach equilibria was determined by spectrophotometry). The molar absorptivities of Cu(PTDITA) and Cu(EGTA) at 12 different wavelengths (400, 425, 600, 615, 625, 630, 650, 665, 680, 700, 725, and 750 nm) were determined by recording the spectra of 4×10^{-4}, 7×10^{-4}, 1×10^{-3}, and 1.5×10^{-3} M solutions (pH = 7.11). For calculation of the equilibrium data, the absorbance values were measured at 12 wavelengths (400, 425, 600, 615, 625, 630, 650, 665, 680, 700, 725, and 750 nm). Formation of the dinuclear Cu_2(PTDITA) complexes was studied by spectrophotometry at a metal-to-ligand ratio of 2:1 in the wavelength range 400−800 nm ($[Cu^{2+}] = 3 \times 10^{-3}$ M, [PTDITA] = 1.5×10^{-3} M, [KCl] = 0.1 M, 25 °C). The spectrophotometric measurements were made with the use of 1.0 cm cells and a Cary 1E spectrophotometer at 25 °C. The protonation and stability constants were calculated with the program *PSEQUAD*.[12]

NMR Experiments. ^{1}H NMR spectra of PTDITA were collected using either a Bruker DRX 400 (9.4 T) or a Bruker DMX 500 (11.75 T) NMR spectrometer. For these experiments, a 0.01 M solution of PTDITA was prepared in H_2O (D_2O was contained in a capillary) and the pH was adjusted by the stepwise addition of a solution of KOH and HCl. The calculations were performed by using the computer program *Micromath Scientist*, version 2.0 (Salt Lake City, UT).

Water Proton Relaxivity Measurements. The water proton longitudinal relaxation rates as a function of the temperature (20 MHz) were measured with a Stelar Spinmaster FFC-2000 spectrometer (Mede, PV, Italy) on about 0.8−1.9 mM aqueous solutions in nondeuterated water. The exact concentrations of

dx.doi.org/10.1021/ic202559h | *Inorg. Chem.* 2012, 51, 2597−2607

Table 1. Protonation Constants of PTDITA, PyMTA, and 1,3,5-Triazine-2,4,6-triamine at 25 °C

	PTDITA (0.1 M KCl)			1,3,5-triazine-2,4,6-triamine (0.1 M KCl)			PyMTA[a] (1.0 M KCl)
method	pH potentiometry	^{1}H NMR	UV	pH potentiometry	^{1}H NMR	UV	pH potentiometry
log K_1^H	8.05 (0.01)	7.91 (0.09)		5.15 (0.02)	5.18 (0.01)	5.06 (0.02)	8.82
log K_2^H	4.71 (0.02)			0.40 (0.06)			7.96
log K_3^H	4.02 (0.02)		3.88 (0.06)				2.57
log K_4^H	3.36 (0.02)						2.20
log K_5^H	3.00 (0.02)						
log K_5^H	1.92 (0.03)						

[a]Reference 7.

gadolinium were determined by measurement of the bulk magnetic suceptibility shifts of a *tert*-BuOH signal on a Bruker Avance 600 spectrometer (14.1 T).[22] The ^{1}H T_1 relaxation times were acquired by the standard inversion–recovery method with a typical 90° pulse width of 3.5 μs, 16 experiments of 4 scans. The reproducibility of the T_1 data was ±5%. The temperature was controlled with a Stelar VTC-91 air-flow heater equipped with a calibrated copper–constantan thermocouple (uncertainty of ±0.1 °C). The proton $1/T_1$ nuclear magnetic relaxation dispersion (NMRD) profiles were measured on a fast-field-cycling Stelar SmartTracer relaxometer over a continuum of magnetic field strengths from 0.00024 to 0.25 T (corresponding to 0.01–10 MHz proton Larmor frequencies). The relaxometer operates under computer control with an absolute uncertainty in $1/T_1$ of ±1%. Additional data points in the range 15–70 MHz were obtained on a a Bruker WP80 NMR electromagnet adapted to variable-field measurements (15–80 MHz proton Larmor frequency) on a Stelar relaxometer.

^{17}O NMR Measurements. Variable-temperature ^{17}O NMR measurements were recorded on a Bruker Avance 600 spectrometer (14.1 T), equipped with a 5 mm probe, by using a D_2O external lock. Experimental settings: spectral width 10 000 Hz, 90° pulse (7 μs), acquisition time 10 ms, 1000 scans, and no sample spinning. Aqueous solutions of the complex (~8 mM) containing 2.0% of the ^{17}O isotope (Cambridge Isotope) were used. The observed transverse relaxation rates, R_2, were calculated from the signal width at half-height.

RESULTS AND DISCUSSION

Solution Equilibria of PTDITA. *Protonation Equilibria of H_4PTDITA and 1,3,5-Triazine-2,4,6-triamine.* The protonation constants of H_4PTDITA, defined by eq 1, have been determined by pH potentiometry, and the log K_i^H values are listed and compared with those of 1,3,5-triazine-2,4,6-triamine and H_4PyMTA (H_4PyMTA = 2,6-pyridinebis(methanamine)-*N*,*N*,*N*′,*N*′-tetraacetic acid; Scheme 1), taken as related model compounds. The results are reported in Table 1 (standard deviations are shown in parentheses).

$$K_i^H = \frac{[H_iL]}{[H_{i-1}][H^+]} \quad (1)$$

where i = 1, 2, ..., 5.

The protonation constants have also been determined by pH ^{1}H NMR and UV-spectrophotometric titrations by recording the chemical shift variation of the nonlabile protons and the absorbances at 225 and 240 nm. The ^{1}H NMR (Figure 1) and UV (Figure 2) titration curves display sharp changes at different pH values, which are related to protonation of the ligand. Because this protonation is fast on the NMR time scale, the chemical shifts of the observed signals represent a weighted average of the shifts of different species involved in a specific protonation step (eq 2)[13]

$$\delta_{H(obs)} = \sum x_i \delta_H^{H_iL} \quad (2)$$

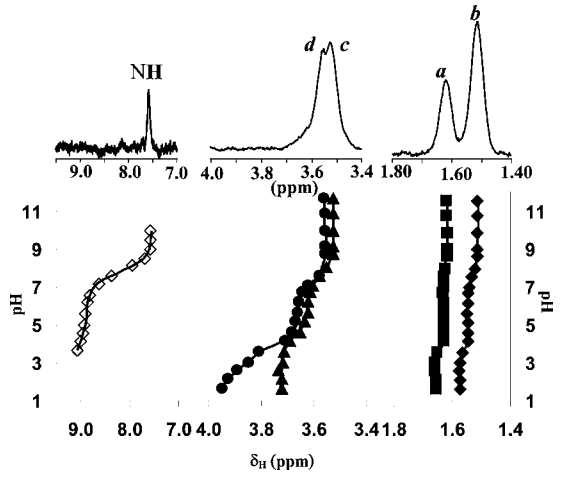

Figure 1. ^{1}H NMR spectrum at pH = 9.00 and titration curves of H_4PTDITA [*NH* (◇), *d* (●), *c* (▲), *b* (■), *a* (◆); *a*–*c* give rise to multiplets at pH > 10; in this case, the center of each multiplet is plotted. [PTDITA] = 0.01 M, [KCl] = 0.1 M, 25 °C].

where $\delta_{H(obs)}$ is the observed chemical shift of a given signal and x_i and $\delta_H^{H_iL}$ are the molar fraction and chemical shift of the involved species, respectively. Similarly, because the absorbance of the ligand includes the absorption of each protonated species, a weighted average of the absorption of these species is observed at each wavelength:[14]

$$A = \sum x_i \varepsilon_H^{H_iL} l \quad (3)$$

where A is the absorbance at a given wavelength and x_i, $\varepsilon_H^{H_iL}$, and l are the molar fraction, molar absorptivity of the species, and path length of the cell, respectively. The observed chemical shifts ($\delta_{H(obs)}$) and absorbance values (A) have been fitted with eqs 2 and 3, respectively (the molar fractions x_i of the different protonated species are expressed with the use of the protonation constants K_i^H). The fits of the experimental data points are shown in Figure 1–4. The obtained log K_i^H values are listed in Table 1.

The protonation scheme of 1,3,5-triazine-2,4,6-triamine has been studied via the pH dependence of the ^{1}H NMR chemical shift of the NH protons and UV spectra of the ligand both reported in the Supporting Information (Figures S1 and S2). The addition of 1 equiv of acid to 1,3,5-triazine-2,4,6-triamine results in the downfield shift of the ^{1}H NMR signal of the NH protons and in the increase of the absorbances at 220 and 237 nm. The first protonation constant obtained from the pH-potentiometric titration (log K_1^H = 5.15) agrees well with the values determined by ^{1}H NMR (log K_1^H = 5.18) and UV spectrophotometric titrations (log K_1^H = 5.06).

dx.doi.org/10.1021/ic202559h | *Inorg. Chem.* 2012, 51, 2597–2607

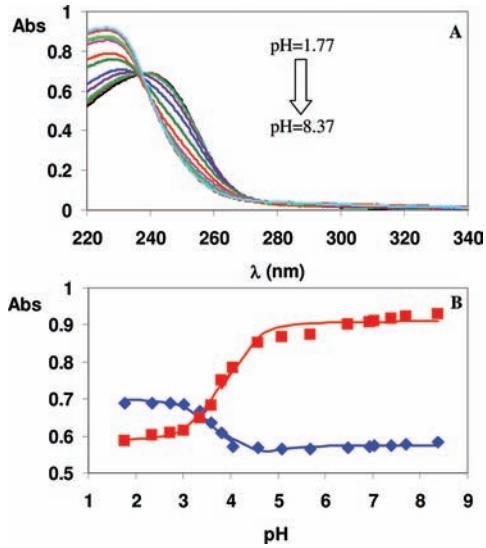

Figure 2. Absorption spectra (pH = 1.77−8.37) (A) and UV-spectrophotometric titration curve (B) of the PTDITA ligand ($Abs_{225\ nm}$ (red ■) and $Abs_{240\ nm}$ (blue ◆), [PTDITA] = 2×10^{-5} M, 0.1 M KCl, 25 °C).

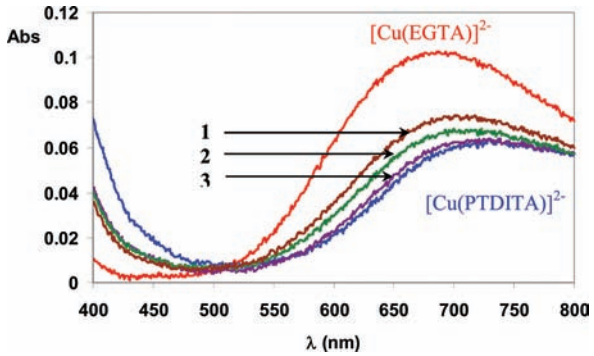

Figure 3. Visible spectra of the $[Cu(EGTA)]^{2-}$, $[Cu(PTDITA)]^{2-}$, and Cu^{2+}/EGTA/PTDITA systems at pH = 7.5: $[Cu(EGTA)^{2-}] = [Cu(PTDITA)^{2-}] = 1.47 \times 10^{-3}$ M; $[Cu^{2+}] = 1.47 \times 10^{-3}$ M, $[PTDITA] = 1.47 \times 10^{-3}$ M, $[EGTA] = 5.03 \times 10^{-3}$ M (**1**); $[Cu^{2+}] = 1.47 \times 10^{-3}$ M, $[PTDITA] = 1.47 \times 10^{-3}$ M, $[EGTA] = 2.25 \times 10^{-3}$ M (**2**); $[Cu^{2+}] = 1.47 \times 10^{-3}$ M, $[PTDITA] = 1.47 \times 10^{-3}$ M, $[EGTA] = 5.1 \times 10^{-4}$ M (**3**); pH = 7.50, [KCl] = 0.1 M, 25 °C.

In order to determine the protonation scheme of PTDITA, the ^{1}H NMR and UV-spectrophotometic titration curve were analyzed simultaneously. In the ^{1}H NMR spectra of PTDITA at pH > 10, the methylene protons of the acetate groups (*d*) and hydrazine NH protons (*e*) give rise to two singlets, while relatively broad multiplets are produced by the methylene protons of the piperidine ring (*a*−*c*).

The addition of 1 equiv of acid to $PTDITA^{4-}$ results in a downfield shift of the signals of the *c*−*e* protons, whereas the signals of the protons *a* and *b* are shifted slightly to higher frequencies. Because the absorption spectra of the ligand were unchanged in the pH range 6.5−9, it can be assumed that the first protonation takes place at the hydrazine distal nitrogen atoms. In the pH range 4−6, the second and third protonation processes slightly shift downfield all proton signals, whereas the absorbance of the peak at 225 nm decreases and that of 240 nm increases significantly. Because in this pH range the signals of the protons *d* are shifted to higher frequencies and the absorbance of the ligand slightly changes, we can assume that

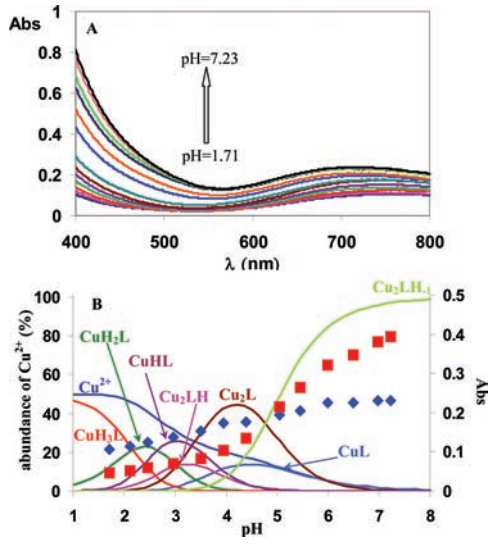

Figure 4. (A) Visible spectra and (B) species distribution diagram and spectrophotometric titration data for the Cu^{2+}(PTDITA) system [$Abs_{450\ nm}$ (red ■), $Abs_{750\ nm}$ (blue ◆), $[Cu^{2+}] = 3 \times 10^{-3}$ M, $[PTDITA] = 1.5 \times 10^{-3}$ M, [KCl] = 0.1 M, 25 °C].

the second protonation takes place at the unprotonated hydrazine distal nitrogen atom. Then, because the absorbance of the ligand is strongly affected by the third protonation process, probably the third proton goes on the piperidine nitrogen atom. Finally, at pH < 4, the signals of the acetate methylene protons are significantly shifted downfield, whereas the absorbance of the ligand is unchanged, confirming that log K_4^H and log K_5^H are related to protonation of the carboxylate groups.

A comparison of the protonation constants of H_4PTDITA with those of PyMTA, obtained in similar media, indicates that the log K_1^H and log K_2^H values of PTDITA are lower, whereas its log K_3^H and log K_4^H values are significantly higher. In summary, the $\sum$ log K_i^H values (Table 1) indicate that the total basicity of PTDITA is somewhat higher than that of PyMTA. Thus, because the donor atoms of the ligand are involved in both protonation and coordination of the metal ions, the total basicity of PTDITA indirectly affects the stability of its metal complexes, which are then expected to be at least as stable as those of PyMTA.

Complexation Properties of PTDITA. The protonation constants of the ligand, the composition, and the protonation and stability constants of the complexes formed with Gd^{3+} and biologically relevant endogenous metal ions (Mg^{2+}, Ca^{2+}, Cu^{2+}, Zn^{2+}) involved in the complex equilibria present in the body fluids have been determined to simulate the behavior in plasma of a Gd^{III}-based CA. The development of suitable plasma models has received renewed attention in recent years,[15,16] and simplified models have been used to predict the concentration of the free Gd^{3+} in blood plasma in the presence of MRI CAs.[1,17,18]

The stability and protonation constants of the metal complexes formed with the PTDITA ligand are defined by eqs 4 and 5:

$$K_{ML} = \frac{[ML]}{[M][L]} \quad (4)$$

dx.doi.org/10.1021/ic202559h | Inorg. Chem. 2012, 51, 2597−2607

Table 2. Protonation and Stability Constants of the Copper(II) and Zinc(II) Complexes with H_4PTDITA, H_4PyMTA, H_3DTPA-BMA, and H_5DTPA (25 °C)

	PTDITA (0.1 M KCl)		PyMTA[a] (1.0 M KCl)		DTPA-BMA[b] (0.15 M NaCl)		DTPA[b] (0.15 M NaCl)	
	Cu^{2+}	Zn^{2+}	Cu^{2+}	Zn^{2+}	Cu^{2+}	Zn^{2+}	Cu^{2+}	Zn^{2+}
log K_{ML}	15.95 (0.02)[c]	15.33 (0.03)	15.69	15.84	16.34	12.42	23.44	17.58
log K_{MHL}	3.78 (0.03)	3.69 (0.01)	3.45	3.81	3.41	4.15	4.63	5.37
log K_{MH_2L}	3.04 (0.02)	2.15 (0.03)			1.46	1.71	2.67	2.38
log K_{MH_3L}	2.18 (0.03)						2.03	
log $K_{MLH_{-1}}$	9.36 (0.03)	10.61 (0.05)			8.95	10.52		11.56
log K_{M_2L}	3.48 (0.04)	2.75 (0.06)			3.95	3.24	6.56	4.33
log K_{M_2LH}	3.34 (0.04)						2.20	
log $K_{M_2LH_{-1}}$	4.77 (0.03)							

[a]Reference 7. [b]Reference 19. [c]Competition reaction between PTDITA and EGTA followed by visible spectrophotometry (0.1 M KCl, 25 °C).

$$K_{MH_iL} = \frac{[MH_iL]}{[MH_{i-1}L][H^+]} \quad (5)$$

where i = 1−3.

The protonation and stability constants of the complexes have been calculated from the titration curves obtained at 1:1 metal-to-ligand concentration ratios. The best fitting was obtained by using the model that includes the formation of both ML and MHL species in equilibrium. The formation of MH_2L and MH_3L complexes was taken into account in the cases of the Cu^{2+}- and Zn^{2+}/PTDITA systems. The titration data of H_4PTDITA in the presence Ln^{3+}, Zn^{2+}, and Cu^{2+} indicate base-consuming processes at pH > 9. These processes can be interpreted by assuming hydrolysis of the metal ion or coordination of the OH^- ion according to eq 6.

$$MLH_{-1} + H^+ \rightleftharpoons ML \quad (6)$$

$$K_{MLH_{-1}} = \frac{[ML]}{[MLH_{-1}][H^+]}$$

The protonation and stability constants of the metal complexes are reported in Table 2 and compared with those of the related complexes with PyMTA. Because of the particularly high stability of $[Cu(PTDITA)]^{2-}$, the determination of its stability constant cannot be carried out by direct pH-potentiometric titration but rather using an appropriate competition reaction. If we assume that log K_{ML} for $[Cu(PTDITA)]^{2-}$ is similar to the value (15.7) for $[Cu(PyMTA)]^{2-}$, then EGTA can represent a suitable chelator for the UV−vis-spectrophotometric competition experiment (log $K_{Cu(EGTA)}$ = 17.2). The reaction (eq 7) has been investigated in the pH range 7−7.5, where both $[Cu(PTDITA)]^{2-}$ and $[Cu(EGTA)]^{2-}$ are present in the equilibria.

$$[Cu(PTDITA)]^{2-} + H_xEGTA \rightleftharpoons [Cu(EGTA)]^{2-} + H_yPTDITA + (x - y)H^+ \quad (7)$$

The absorption spectra obtained for the systems $[Cu(PTDITA)]^{2-}$, $[Cu(EGTA)]^{2-}$, and Cu^{2+}/PTDITA/EGTA are shown in Figure 3.

The positions of the absorption bands and the molar absorptivities of $[Cu(PTDITA)]^{2-}$ and $[Cu(EGTA)]^{2-}$ differ considerably. The maxima of the absorption bands of $[Cu(PTDITA)]^{2-}$ and $[Cu(EGTA)]^{2-}$ fall at 730 and 680 nm, respectively. The isosbestic point indicates the presence of two absorbing species, $[Cu(PTDITA)]^{2-}$ and $[Cu(EGTA)]^{2-}$, in the pH range investigated. A value of 15.95 was obtained for log K_{ML} of $[Cu(PTDITA)]^{2-}$ by using the protonation constants of EGTA (log K_1^H = 9.43 (0.01), log K_2^H = 8.82 (0.01), log K_3^H = 2.77 (0.01), log K_4^H = 2.06 (0.01), [KCl] = 0.1 M, 25 °C) and PTDITA (Table 1) and the stability constant of $[Cu(EGTA)]^{2-}$ (log $K_{Cu(EGTA)}$ = 17.22 (0.02), [KCl] = 0.1 M, 25 °C).

To obtain information about the formation and stability of dinuclear complexes in the Zn^{2+}/PDTITA and Cu^{2+}/PTDITA systems, pH-potentiometric titrations were carried out also at a 2:1 metal-to-ligand ratio. The protonation and stability constants were calculated simultaneously from the titration curves obtained at 1:1 and 2:1 metal-to-ligand concentration ratios by using a model that includes formation of the ML, MHL, MH_2L, MH_3L, MLH_{-1}, M_2L, M_2LH, and M_2LH_{-1} species. The equilibrium constants for formation of the dinuclear metal complexes are given by

$$ML + M \overset{K_{M_2L}}{\rightleftharpoons} M_2L \quad (8)$$

$$K_{M_2L} = \frac{[M_2L]}{[ML][M]}$$

$$M_2L + H \overset{K_{M_2LH}}{\rightleftharpoons} M_2LH \quad (9)$$

$$K_{M_2LH} = \frac{[M_2LH]}{[M_2L][H^+]}$$

$$M_2LH_{-1} + H^+ \overset{K_{M_2LH_{-1}}}{\rightleftharpoons} M_2L \quad (10)$$

$$K_{M_2LH} = \frac{[M_2L]}{[M_2LH_{-1}][H^+]}$$

The log K_{ML} values of the zinc(II) and copper(II) complexes of PTDITA are very similar to those of PyMTA, probably as a result of the similarity in the nature of the donor atoms and coordination polyhedra. However, PTDITA can form two protonated complexes, which indicates the presence of at least two free donor atoms. The presence of free donor atoms also explains formation of the dinuclear M_2L, M_2LH, and M_2LH_{-1} species, which we need to take into account for interpreting the pH-potentiometric titration data (Table 2).

The visible spectra of the Cu^{2+}/PTDITA system show significant changes with the pH. In the pH range 1.8−4.0, coordination of the second Cu^{2+} ion and formation of the Cu_2(PTDITA) species result in a new absorption band at

dx.doi.org/10.1021/ic202559h | Inorg. Chem. 2012, 51, 2597−2607

Table 3. Protonation and Stability Constants of Mg^{2+}, Ca^{2+}, and Ln^{3+} Complexes with H_4PTDITA, H_4PyMTA, H_3DTPA-BMA, and H_5DTPA Ligands (25 °C)

	PTDITA (0.1 M KCl)			PyMTA[a] (1.0 M KCl)	DTPA-BMA[c] (0.1 M KCl)		DTPA[c] (0.1 M KCl)	
	log K_{ML}	log K_{MHL}	log $K_{MLH_{-1}}$	log K_{ML}	log K_{ML}	log K_{MHL}	log K_{ML}	log K_{MHL}
Mg^{2+}	8.37 (0.03)						9.27	6.85
Ca^{2+}	9.79 (0.03)	3.86 (0.02)		9.43	7.17[d]	4.45[d]	10.75[d]	6.11[d]
La^{3+}	16.12 (0.05)	2.91 (0.05)	10.73 (0.08)	15.5[b]	14.55		19.49	2.60
Gd^{3+}	18.49 (0.02)	2.81 (0.05)	10.43 (0.08)	18.6	16.38		22.46	2.39
Lu^{3+}	17.15 (0.03)	2.97 (0.03)	9.97 (0.06)	18.0[b]	17.06		22.44	2.18
pGd[e]		18.6		17.5	16.0		19.1	

[a]Reference 7. [b]Reference 20. [c]References 21 and 19. Gd(DTPA-BMA): log K_{GdL} = 16.64. Gd(DTPA): log K_{GdL} = 22.03, log K_{GdHL} = 1.96 (0.15 M NaCl, 25 °C). [d]Reference 21 (0.1 M NaCl, 25 °C). [e]pGd = −log $[Gd^{3+}]_{free}$, $[Gd^{3+}]_{tot} = 10^{-6}$ M, $[L]_{tot} = 10^{-5}$ M.[7]

around 400 nm. However, formation of the dinuclear complex has no effect on the absorption band at 750 nm (the absorbance only slightly increases). Above pH = 4.0, coordination of the OH^- ion and formation of the Cu_2LH_{-1} species occur, resulting in a ca. 25 nm blue shift of the absorption band at 750 nm and a further increase of the absorbance at 400 nm (Figure 4A). The absorbance values of the 2:1 Cu^{2+}(PTDITA) system as a function of the pH are in good agreement with the species distribution curves calculated from the equilibrium data determined by pH potentiometry (Figure 4B).

The stability constants of the Mg^{II}-, Ca^{II}-, and Ln^{III}(PTDITA) complexes (Ln = La, Gd, and Lu) are comparable with those of the corresponding complexes of PyMTA (Table 3). log K_{ML} of $[Ca(PTDITA)]^{2-}$ is about 0.5 order of magnitude higher than that of $[Ca(PyMTA)]^{2-}$, probably because of a better size match between the Ca^{2+} ion and the rigid cavity of PTDITA. The smaller Mg^{2+} cation does not fit well in the cavity of the ligand, and the log K_{ML} value is lower than that of $[Ca(PTDITA)]^{2-}$. At pH < 3, one carboxylate group in both the Ca^{II}- and Ln^{III}(PTDITA) complexes is protonated with the log K_{MHL} values reported in the range 2.81−3.86 (Table 3).

The stability constants of the $[Ln(PTDITA)]^-$ complexes are about 3−4 orders of magnitude lower than those of the corresponding $[Ln(DTPA)]^{2-}$ complexes (H_4DTPA = diethylenetriamine-*N*,*N*,*N*′,*N*″,*N*″-pentaacetic acid), comparable to those of the $[Ln(PyMTA)]^-$ complexes, and even higher than those of Ln(DTPA-BMA) complexes (H_3DTPA-BMA = 1,7-bis(methylcarbamoylmethyl)-1,4,7-triazaheptane-1,4,7-triacetic acid; Scheme 2).[19−21] The log K_{LnL} value of the $[Ln(PTDITA)]^-$ complexes increases from La^{3+} to Gd^{3+}, and then it markedly decreases for Lu^{3+} (Table 3). This behavior is quite similar to that observed for the $[Ln(PyMTA)]^-$ complexes, although the decrease of log K_{ML} for the heavier lanthanides is more pronounced for PTDITA. This is an effect of the fairly rigid coordination sphere of the donor atoms of PTDITA, which cannot efficiently encapsulate the larger and smaller members of the lanthanide series.

The Gd^{III}-based MRI CAs may be involved in exchange reactions with endogenous metal ions and ligands in body fluids. The toxicity of the CA strongly depends on the extent of such transmetalation reactions. To estimate the Gd^{3+} binding properties of the polyaminocarboxylate ligands under physiological conditions, Cacheris et al. introduced the selectivity constant (K_{sel}).[17] This is a conditional stability constant that

Scheme 2. Chemical Structure of Ligands Discussed in the Text

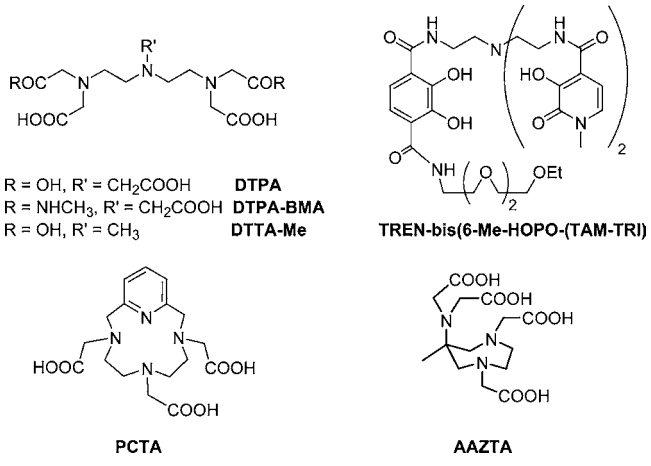

takes into account the possible side reactions of the ligand with H^+, Zn^{2+}, Cu^{2+}, and Ca^{2+}:

$$K_{sel} = \frac{K_{GdL}}{\alpha_L^H + \alpha_L^{Cu} + \alpha_L^{Zn} + \alpha_L^{Ca}} \quad (11)$$

Near physiological conditions (pH ≈ 7.4), the complexes formed are GdL, CaL, CaHL, CuL, Cu_2L, Cu_2LH_{-1}, ZnL, ZnHL, and Zn_2L and the α values can be expressed as follows:

$$\alpha_L^{Ca} = K_{CaL}[Ca^{2+}] + K_{CaL}K_{CaHL}[Ca^{2+}][H^+] \quad (12)$$

$$\alpha_L^{Cu} = K_{CuL}[Cu^{2+}] + K_{CuL}K_{Cu_2L}[Cu^{2+}]^2 + \frac{K_{CuL}K_{Cu_2L}[Cu^{2+}]^2}{K_{Cu_2LH_{-1}}[H^+]} \quad (13)$$

$$\alpha_L^{Zn} = K_{ZnL}[Zn^{2+}] + K_{ZnL}K_{ZnHL}[Zn^{2+}][H^+] + K_{ZnL}K_{Zn_2L}[Zn^{2+}]^2 \quad (14)$$

The concentration of CaHL for $[Ca(PTDITA)]^{2-}$, $[Ca(PyMTA)]^{2-}$, and $[Ca(DTPA-BMA)]^-$ is very low at pH = 7.4, and thus the second term in eq 12 can be neglected. Because the dinuclear $[Cu_2(PyMTA)]$, $[Cu_2(PyMTA)H_{-1}]^-$, $[Cu_2(DTPA-BMA)H_{-1}]$, and $[Cu_2(DTPA)H_{-1}]^{2-}$ complexes were not detected, the second and third terms for PyMTA and the third term for DTPA-BMA and DTPA can be neglected in eq 13. In eq 14, the second term for PTDITA and DTPA-BMA and the second and third terms for PyMTA can also be

dx.doi.org/10.1021/ic202559h | Inorg. Chem. 2012, 51, 2597−2607

neglected because of the low protonation constant values of the related zinc(II) complexes and the absence of formation of the dinuclear $[Zn_2(PyMTA)]$ species, respectively.

According to the plasma model developed by May et al., the concentrations of the exchangeable Ca^{2+}, Cu^{2+}, and Zn^{2+} ions are 1.5×10^{-3} M, 1×10^{-6} M, and 1.6×10^{-5} M, respectively.[15,16] By taking into account the concentration of the exchangeable Cu^{2+} and Zn^{2+} ions and the stability constant of the Gd^{III}, Ca^{II}, Cu^{II}, and Zn^{II} complexes formed with PTDITA, PyMTA, DTPA-BMA, and DTPA, the K_{sel} values are calculated for $[Gd(PTDITA)]^-$, $[Gd(PyMTA)]^-$, Gd(DTPA-BMA), and $[Gd(DTPA)]^{2-}$ and are shown in Table 4. These

Table 4. K_{sel} Values of $[Gd(PTDITA)]^-$, $[Gd(PyMTA)]^-$, Gd(DTPA-BMA), and $[Gd(DTPA)]^{2-}$ at pH = 7.4 ($[Cu^{2+}] = 1 \times 10^{-6}$ M, $[Zn^{2+}] = 1.6 \times 10^{-5}$ M, $[Ca^{2+}] = 1.5 \times 10^{-3}$ M, 25 °C)[a]

	K_{sel}
$[Gd(PTDITA)]^-$	6.78×10^7
$[Gd(PyMTA)]^-$	3.45×10^7
Gd(DTPA-BMA)	3.41×10^6
$[Gd(DTPA)]^{2-}$	2.85×10^4

[a]The $\log K_{ML}$ values used for K_{sel} calculation were determined for DTPA and DTPA-BMA in a 0.15 M NaCl solution and for PTDITA and PyMTA in 0.1 and 1.0 M KCl, respectively. The K_{sel} value is not influenced by this difference because the terms considering the different ionic strengths are neglected in the calculation.

K_{sel} values indicate that, near physiological conditions, the presence of the 1,3,5-triazine ring increases the selectivity of the PTDITA ligand for Gd^{3+} ion compared to PyMTA, DTPA-BMA, and DTPA. The relatively high K_{sel} value of the PTDITA ligand can be accounted for by the low values of α_L^H, α_L^{Cu}, and α_L^{Zn} terms due to the low second protonation constant of the ligand and to the lower stability of $[Cu(PTDITA)]^{2-}$ and $[Zn(PTDITA)]^{2-}$. It must be highlighted that, although the selectivity of PTIDTA for Gd^{3+} and other lanthanides is relatively high, their in vivo use is possible only if the kinetic inertness of the Ln(PTIDTA) complexes is also high, higher than that, e.g., of the Ln(DTPA) complexes.

In order to study $[Gd(PTDITA)]^-$ complex formation and confirm the presence of the species observed by pH potentiometry, the UV spectra of the Gd^{3+}/PTDITA system at different pH values were also recorded. Species distribution and absorption spectra obtained at a 1:1 metal-to-ligand ratio for the Gd^{3+}/PTDITA system are shown in Figure 5. The UV spectra of the Gd^{3+}/PTDITA system show significant changes upon complex formation: in the pH range 1.8−3.5, the absorbance at 225 nm increases, whereas the absorbance at 253 nm decreases, respectively. Around pH = 3, Gd(HPTDITA) is the predominant species in solution and its deprotonation has no effect on the absorbance values, indicating that protonation of the complex takes place relatively far away from the chromophore. As was already observed, protonation probably occurs at one carboxylate group, as confirmed by the value of the protonation constant ($\log K_{GdHL} = 2.81$). In the pH range 3.5−9, the presence of $[Gd(PTDITA)]^-$ results in invariance of the UV spectra. At pH > 9, the absorbance at 225 nm increases with an increase of the pH, probably because of coordination of a OH^- ion and formation of $[Gd(PTDITA)OH]^{2-}$ species. The absorbance values as a function of the pH are in good agreement with the species distribution curves of the Gd^{3+}/

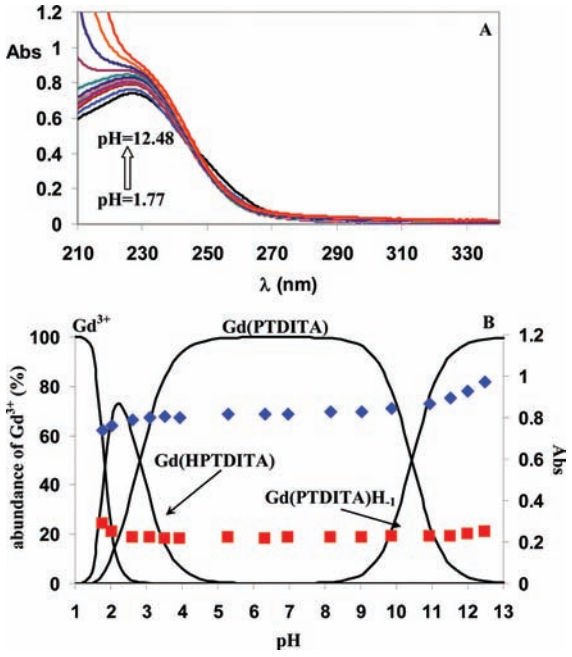

Figure 5. Absorption spectra (A) and the species distribution curves and UV absorbance values of the Gd^{3+}(PTDITA) system (B) [$Abs_{225\ nm}$ (red ■) and $Abs_{253\ nm}$ (blue ◆), $[Gd^{3+}] = [PTDITA] = 2 \times 10^{-5}$ M, [KCl] = 0.1 M, 25 °C].

PTDITA system, which were calculated from the equilibrium data determined by pH potentiometry.

Relaxometric Properties of $[Gd(PTDITA)(H_2O)_2]^-$. The relaxivity r_1 represents the increase in the longitudinal nuclear magnetic relaxation rate of the water protons normalized to a 1 mM aqueous solution of a paramagnetic probe. It depends on the magnetic field strength, temperature, and several important physicochemical parameters of the metal complex that describe the magnetic coupling between the solvent nuclei and Gd^{3+}. The r_1 value of $[Gd(PTDITA)(H_2O)_2]^-$, measured at 20 MHz, 25 °C, and pH = 6.8, was found to be 10.2 ± 0.1 mM^{-1} s^{-1}. This relaxivity value is significantly higher than that of the currently used MRI CAs such as $[Gd(DTPA)(H_2O)]^-$ and $[Gd(DOTA)(H_2O)]^-$ ($r_1 \sim 4.7$ mM^{-1} s^{-1} under identical experimental conditions). Because the molecular dimensions of all of these complexes are quite comparable, the r_1 difference is likely associated with a higher number of *inner-sphere* H_2O molecules in Gd(PTDITA), i.e., $q = 2$ vs 1 for Gd(DOTA) and Gd(DTPA). On the other hand, a relaxivity value of 10.2 mM^{-1} s^{-1} is also higher than the values measured for other $q = 2$ complexes that lie in the range from ∼6.0 to 8.9 mM^{-1} s^{-1} (Table 5). To gain more insight into the physicochemical characteristics of this novel $q = 2$ gadolinium(III) complex, detailed ^1H and ^{17}O NMR relaxometric studies were carried out.

pH Dependence. The pH dependence of r_1 is reported in Figure 6a, together with the species distribution diagram for the Gd^{3+}/PTDITA system. In the pH range 1.3−2, the relaxivity decreases from 13 to 10.1 mM^{-1} s^{-1} following formation of both $[Gd(PTDITA)(H_2O)_2]^-$ and its protonated form. In the region 3 < pH < 9, the complete formation of $[Gd(PTDITA)(H_2O)_2]^-$ and the disappearance of its protonated species are not associated with relaxivity changes. On the other hand, r_1 further decreases at pH > 9 and reaches a value of ca. 6 mM^{-1} s^{-1} at pH = 12. Such a decrease has often been observed in

dx.doi.org/10.1021/ic202559h | Inorg. Chem. 2012, 51, 2597−2607

Table 5. Parameters Obtained from the Simultaneous Analysis of ^{1}H NMRD Profiles and ^{17}O NMR Data (14.1 T) for the Gd^{3+} Complexes of PTDITA and Related Ligands (PCTA,[8] DO3A,[8] TREN-bis[6-Me-HOPO-(TAM-TRI)],[22] and AAZTA[6])

parameter	PTDITA[a]	PCTA	DO3A	TREN-bis[6-Me-HOPO-(TAM-TRI)]	AAZTA
$^{20}r_1^{298}$ (mM^{-1} s^{-1})	10.2	6.9	6.0	8.9	7.1
Δ^2 ($\times 10^{19}$ s^{-2})	2.5 ± 0.2	2.8	4.6	8.7	2.2
τ_V^{298} (ps)	22 ± 2	28	14	24	31
k_{ex}^{298}($\times 10^6$ s^{-1})	3.3 ± 0.2	14.3	6.4	52.6	11.1
τ_R^{298} (ps)	105 ± 6	70	66	118	74
q	2[b]	2	1.9	2	2
r (Å)	3.0[b]	3.1	3.15	3.10	3.10
E_V (kJ mol^{-1})	1.0[b]		2.0	2.0	
$\Delta H^{\ddagger}_M$ (kJ mol^{-1})	37.7 ± 1.1	45	44	25.9	
$A/\hbar$ ($\times 10^6$ rad s^{-1})	−3.3 ± 0.2	−3.8	−3.8	−3.8	−3.8

[a]For the parameters a, ^{298}D, E_R, and E_D, the values of 3.8 Å, 2.24 × 10^{-5} cm^2 s^{-1}, 18, and 21 kJ mol^{-1}, respectively, were used. [b]Fixed in the fitting procedure.

other q = 2 complexes, and it has been explained as a result of (i) partial water displacement by carbonate anions present in the aerated solution, (ii) hydrolysis of the complex, and (iii) slowing of the water exchange rate following deprotonation of an *inner-sphere* H_2O molecule or coordination of the OH^- ion. The complete reversibility of the behavior excludes the occurrence of hydrolysis.

NMRD Profiles and ^{17}O NMR Data. The magnetic field dependence of the relaxivity, the so-called NMRD profile, has been measured at 25 and 37 °C in the proton Larmor frequency range 0.01−70 MHz, corresponding to magnetic field strengths varying between 2.34 × 10^{-4} and 1.64 T (Figure 6b). The profiles have the typical shape of low-molecular-weight complexes, with a plateau at low fields, a dispersion around 3−4 MHz, and another plateau in the high-field region (>20 MHz). The lower values of the relaxivity at 37 °C over the entire range of proton Larmor frequencies indicate that r_1 is not limited by the water exchange rate but rather by the fast rotational motion of the complex. More accurate information on the kinetics of the water exchange is obtained by measuring the temperature dependence of the ^{17}O NMR transverse relaxation rate, R_2. The data were measured at 14.1 T on a 8 mM solution of the complex at neutral pH. The R_2 values increase with the temperature from 275 to 315 K, where a maximum is observed and then they decrease at higher temperatures (Figure 6c). This profile is rather typical of Gd^{3+} chelates characterized by intermediate values of the water exchange lifetime (τ_M ∼ 200−600 ns) as for Gd(DTPA) and Gd(DOTA).

The experimental data, NMRD and ^{17}O NMR, were fitted simultaneously according to the established theory of paramagnetic relaxation expressed in terms of the SBM[23] and Freed's[24] equations for the *inner-* and *outer-sphere* proton relaxation mechanisms, respectively, and of the Swift−Connick theory for ^{17}O relaxation.[25] The number of coordinated H_2O molecules was fixed to two, the distance of closest approach of the *outer-sphere* H_2O molecules to Gd^{3+} was set to 3.8 Å, a typical value for small metal chelates, and for the relative diffusion coefficient D, the standard value of 2.24 × 10^{-5} cm^2 s^{-1} (298 K) was used. The Gd−water proton distance r and the rotational correlation time τ_R are strongly correlated parameters, and therefore one of the two needs to be fixed. According to the results of a pulsed ENDOR study by Caravan et al.,[26] the r values for selected DTPA- and DOTA-like gadolinium(III)

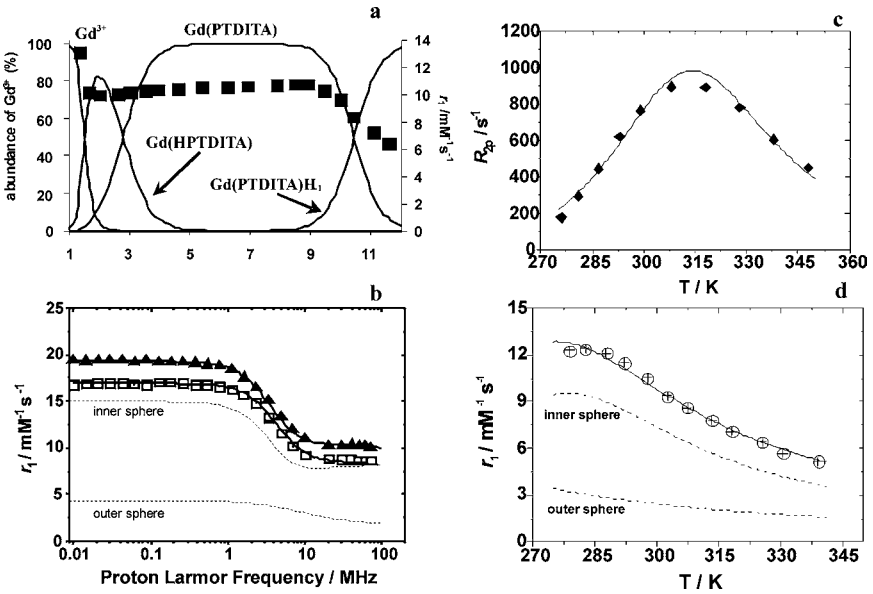

Figure 6. (a) Plot of ^{1}H relaxivity r_{1p} at 20 MHz and 298 K for $[Gd(PTDITA)(H_2O)_2]^-$ and the species distribution diagram of the Gd^{3+}/PTDITA system as a function of the pH ($[Gd^{3+}]$ = [PTDITA] = 1 × 10^{-3} M, [KCl] = 0.1 M, 20 MHz, 25 °C). (b) $1/T_1$ ^{1}H NMRD relaxation data for $[Gd(PTDITA)(H_2O)_2]^-$ at pH = 7.2: 298 K (▲); 310 K (□). The solid lines represent the best results of the fitting to the experimental points (see Table 3). The *inner-* and *outher-sphere* contributions to the total relaxivity are also shown. (c) Temperature dependence of the transverse water ^{17}O relaxation rates at 14.1 T and pH = 7 for a 8 mM solution of $[Gd(PTDITA)(H_2O)_2]^-$. (d) Temperature dependence of the longitudinal water proton relaxivity at 20 MHz and pH = 7.

dx.doi.org/10.1021/ic202559h | *Inorg. Chem.* 2012, 51, 2597−2607

complexes fall in the range 3.0−3.2 Å. In our case, the best result was obtained by fixing r to the value of 3.0 Å. By using a longer value, an unrealistic τ_R value is obtained and the quality of the fit deteriorates. The best-fit parameters are listed in Table 5 and compared with those of related q = 2 gadoliniun complexes of similar size. The rotational correlation time τ_R is intermediate between the corresponding values of Gd(AAZTA) and Gd(TREN-bis[6-Me-HOPO-(TAM-TRI)]) (Scheme 2), reflecting their relative molecular weight. The τ_M value of 299 ns obtained for Gd(PTDITA) (298 K) is 2 times that of Gd(DO3A) and 5 times longer than that reported for Gd(PCTA), in spite of the fact that Gd(PTDITA) has one negative charge, whereas the others are neutral. On the other hand, this value is similar to those measured for the anionic complexes Gd(DTPA) and Gd(DOTA). Of course, an effect of the triazine ring on the relatively slow water exchange cannot be excluded. The parameters associated with the electronic relaxation are Δ^2 and τ_V: their values for Gd(PTDITA) are quite similar to those found for Gd(PCTA), Gd(DO3A), and Gd(AAZTA), whereas Δ^2 is more than 3 times longer for Gd(TREN-bis[6-Me-HOPO-(TAM-TRI)]), indicating a faster electronic relaxation.

Temperature Dependence. The temperature dependence of $[Gd(PTDITA)(H_2O)_2]^-$ was measured at 20 MHz over the range 274−340 K and is shown in Figure 6d. The curve through the experimental data and the *inner-* and *outer-sphere* contributions to the overall relaxivity were calculated by using the parameters of Table 5. It is clearly seen that, at $T \leq 285$ K, τ_M becomes so long as to limit the inner-sphere relaxivity and then r_1. However, at physiological temperature (310 K), the relaxivity (8.1 mM^{-1} s^{-1}) is only limited by the rotational correlation time.

Anion Interaction. The two inner-sphere H_2O molecules of q = 2 complexes like Gd(DO3A) and Gd(PCTA) can rather easily be displaced by the anions present in the human plasma such as carbonate (~25 mM), phosphate (~1.1 mM), or citrate (~0.11 mM) with formation of the ternary adducts of lower hydration state and then lower relaxivity.[13,14,27−30] In a few other cases, such as Gd(AAZTA) or Gd(DTTA-Me) (Scheme 2), the adduct formation is much more difficult and the effect on the relaxivity of the physiological concentration of oxoanions is negligible.[6,31] We investigated the changes in the relaxivity of $[Gd(PTDITA)(H_2O)_2]^-$ as a function of increasing concentration of carbonate, phosphate, and citrate up to 60 equiv, at 20 MHz and 25 °C.

The data are reported in Figure 7, where the ratio r_1/r_1^0 (r_1^0 = initial relaxivity) is plotted as a function of the number of equivalents of the added anion. The addition of citrate to the solution of $[Gd(PTDITA)(H_2O)_2]^-$ resulted in a monotonous decrease of the relaxivity up to about 34% (r_1 = 6.7 mM^{-1} s^{-1}) in the presence of 60 equiv of the anion. The binding interaction is then very weak compared to, for example, Gd(EDTA), where a log$K$ of 3.56 was found for the ternary complex with citrate.[32] Both the presence of a negative charge and a possible relative position of the two bound H_2O molecules not suitable for anion binding in a bidentate manner could be responsible of the weak interaction. In the presence of phosphate or carbonate, the relaxivity of $[Gd(PTDITA)(H_2O)_2]^-$ increases up to ~10% for a [anion]/$[Gd(PTDITA)(H_2O)_2]^-$ value of 10 and then it remains constant. From these data, we can estimate log $K \sim 2.2$ for formation of these ternary complexes. Some anions, like phosphate, can displace a single H_2O molecule and bind the complexes in a monodentate

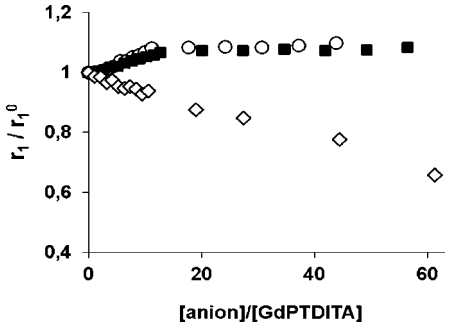

Figure 7. Plot of the observed relaxation rate (pH = 7.4, 0.1 M KCl, 20 MHz, 25 °C) of $[Gd(PTDITA)(H_2O)_2]^-$, normalized to the initial value, as a function of $[PO_4^{3-}]_{tot}/[Gd(PTDITA)(H_2O)_2]^-$ (■), $[CO_3^{2-}]_{tot}/[Gd(PTDITA)(H_2O)_2]^-$ (○), and $[Cit]_{tot}/[Gd(PTDITA)(H_2O)_2]^-$ (◇).

mode. Moreover, formation of the ternary complex can be accompanied by organization of a well-defined *second sphere* of hydration that can make a significant contribution to the relaxivity. This was clearly evidenced in the case of the adducts of triamide DOTA derivatives with fluoride and phosphate.[27] It was shown that the contribution to the relaxivity of the *second-sphere* H_2O molecules can be considerable and comparable to that arising from one inner-sphere H_2O molecule. In fact, in spite of the decrease of q from 2 to 1, the relaxivity of the ternary complex of Gd(PTDITA) with phosphate is slightly higher than that of the free complex over the entire range of magnetic field strengths (Figure 8). As was reported before,

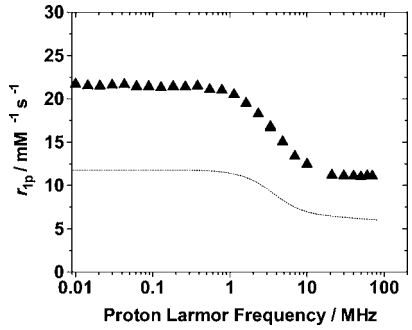

Figure 8. $1/T_1$ NMRD profile of the ternary complex of Gd(PTDITA) with phosphate at 25 °C. The lower dashed curve represents the calculated profile of Gd(PTDITA) by assuming q = 1.

besides a lengthening of τ_R in the ternary complex, an increase of k_{ex} is induced by the increased overall negative charge of the complex and by the increased steric interaction at the water coordination site that might destabilize the nine-coordinate ground state, then lowering the activation energy for the exchange (dissociative) process.[27,29] For example, upon formation of a ternary complex with phosphate, the exchange lifetime of a triamide derivative of Gd(DO3A) decreases from 1.5 to 0.56 μs, at 298 K.[27]

The lower dashed curve in Figure 8 represents the calculated NMRD profile of the hypothetical Gd(PTDITA) complex with q = 1. The difference between the experimental and calculated profiles provides a rough estimation of the contribution of the second hydration sphere. This contribution corresponds to that of two hydrogen-bonded H_2O molecules at a mean distance of 3.4 Å from Gd^{3+}, in accordance with previous analyses.[27,33]

dx.doi.org/10.1021/ic202559h | Inorg. Chem. 2012, 51, 2597−2607

CONCLUSIONS

We have herein reported a complete solution study of the triazine-based heptadentate ligand H_4PTDITA featuring a piperidine ring in position 6 and two hydrazinodiacetate moieties in positions 2 and 4. The protonation constants and thermodynamic stability constants of the complexes of H_4PTDITA with Mg^{2+}, Ca^{2+}, Cu^{2+}, Zn^{2+}, La^{3+}, Gd^{3+}, and Lu^{3+} have been determined by pH potentiometry, UV spectrophotometry, and ^{1}H NMR spectroscopy. The results reported indicate that this ligand forms complexes with thermodynamic stability quite similar to that of the pyridine-based ligand PyMTA, which presents a similar coordination sphere. log K_{GdL} has been determined to be 18.49; thus, the $Gd(PTDITA)^-$ complex cannot be considered for in vivo applications, although the log K_{GdL} value is higher than that reported for the clinically approved Gd(DTPA-BMA). However, because the total basicity of PTDITA is higher than that of comparable ligands such as PyMTA, also the conditional stability constant, pGd, is higher (18.6), almost reaching the value observed for DTPA (19.1). Interestingly, also the selectivity constant (K_{sel}) of $Gd(PTDITA)^-$ is higher than that of other considered Gd^{3+} complexes (PyMTA, DTPA-BMA, and DTPA). Therefore, near physiological conditions, the presence of the 1,3,5-triazine ring increases the selectivity of the PTDITA ligand for the Gd^{3+} ion mainly because of the relatively low second protonation constant of the ligand and to the lower stability of the $[Cu(PTDITA)]^{2-}$ and $[Zn(PTDITA)]^{2-}$ complexes.

A full relaxometric characterization of the $Gd(PTDITA)^-$ complex in aqueous solution has also been performed, showing the presence of two H_2O molecules in the inner coordination sphere of the Gd^{3+} ion and a relaxivity value (10.2 mM^{-1} s^{-1} at 20 MHz and 298 K), stable over a wide pH range, higher than that observed for other q = 2 gadolinium complexes. Measurement of the relaxivity dependence on the temperature and magnetic field strength together with temperature-dependent ^{17}O NMR data confirms these results and allows extrapolation of the various relaxometric data. One of the two inner-sphere H_2O molecules in $Gd[(PTDITA)(H_2O)_2]^-$ has been shown to be displaced by a high concentration of citrate anions, showing a lowering of r_1 down to 35% with the addition of 60 equiv of the anion. Phosphate and carbonate also displace one H_2O molecule, causing though a 10% increase of r_1 due to the large increase of the second-sphere contribution to the relaxivity.

ASSOCIATED CONTENT

Supporting Information

NMR and UV experiments on 1,3,5-triazine-2,4,6-triamine, ^{1}H NMR and absorption spectra, and titration curves. This material is available free of charge via the Internet at http://pubs.acs.org.

AUTHOR INFORMATION

Corresponding Author

*E-mail: mczsozso@yahoo.co.uk (Z.B.), mauro.botta@mfn.unipmn.it (M.B.).

Notes

The authors declare no competing financial interest.

ACKNOWLEDGMENTS

The authors are thankful for the Hungarian Scientific Research Fund (OTKA PD-83253), the EU FP6 European Imaging Laboratories, and Project TÁMOP 4.2.1./B-09/1/KONV-2010-0007 implemented through the New Hungary Development Plan, cofinanced by the European Social Fund and the European Regional Development Fund, for financial support of this work (Z.B.). M.B., G.B.G., and L.T. thank Regione Piemonte (PIIMDMT and Nano-IGT projects) and MIUR (PRIN 2009) for their support. This work was carried out in the frame of the EU COST Action D38.

REFERENCES

(1) Bunzli, J.-C. G.; Choppin, G. R. In *Lanthanide Probed in Life, Chemical and Earth Sciences*; Bunzli, J.-C. G., Choppin, G. R., Eds.; Elsevier: Amsterdam, The Netherlands, 1989.

(2) Tóth, É.; Helm, L. Merbach, A. E. In *The Chemistry of Contrast Agents in Medical Magnetic Resonance Imaging*; Tóth, É., Merbach, A. E., Eds.; John Wiley & Sons: Chichester, U.K., 2001.

(3) (a) Caravan, P.; Ellison, J. J.; McMurry, T. J.; Lauffer, R. B. *Chem. Rev.* **1999**, *99*, 2293. (b) Aime, S.; Botta, M.; Terreno, E. *Adv. Inorg. Chem.* **2005**, *57*, 173.

(4) Datta, A.; Raymond, K. N. *Acc. Chem. Res.* **2009**, *42*, 938.

(5) Costa, J.; Toth, É.; Helm, L.; Merbach, A. E. *Inorg. Chem.* **2005**, *44*, 4747. Livramento, J. B.; Helm, L.; Sour, A.; O'Neil, C.; Merbach, A. E.; Toth, É. *Dalton Trans.* **2008**, 1195. Ruloff, R.; van Koten, G.; Merbach, A. E. *Chem. Commun.* **2004**, 842.

(6) Aime, S.; Calabi, L.; Cavallotti, C.; Gianolio, E.; Giovenzana, G. B.; Losi, P.; Maiocchi, A.; Palmisano, G.; Sisti, M. *Inorg. Chem.* **2004**, *43*, 7588. Baranyai, Z.; Uggeri, F.; Giovenzana, G. B.; Benyei, A.; Brucher, E.; Aime, S. *Chem.—Eur. J.* **2009**, *15*, 1696. Gugliotta, G.; Botta, M.; Tei, L. *Org. Biomol. Chem.* **2010**, *8*, 4569.

(7) Pellegatti, L.; Zhang, J.; Drahos, B.; Villette, S.; Suzenet, F.; Guillaumet, G.; Petoud, S.; Tóth, É. *Chem. Commun.* **2008**, 6591–6593. Laurent, S.; Vander Elst, L.; Wautier, M.; Galaup, C.; Muller, R. N.; Picard, C. *Bioorg. Med. Chem. Lett.* **2007**, *17*, 6230.

(8) Aime, S.; Botta, M.; Geninatti Crich, S.; Giovenzana, G. B.; Pagliarin, R.; Sisti, M.; Terreno, E. *Magn. Reson. Chem.* **1998**, *36*, S200.

(9) Tei, L.; Benzi, M.; Kielar, F.; Botta, M.; Cavallotti, C.; Giovenzana, G. B.; Aime, S. *Helv. Chim. Acta* **2009**, *92*, 2414–2426. Delli Castelli, D.; Terreno, E.; Carrera, C.; Giovenzana, G. B.; Mazzon, R.; Rollet, S.; Visigalli, M.; Aime, S. *Inorg. Chem.* **2009**, *47*, 2928.

(10) Imperio, D.; Giovenzana, G. B.; Law, G.-L.; Parker, D.; Walton, J. W. *Dalton Trans.* **2010**, *39*, 9897.

(11) Irving, H. M.; Miles, M. G.; Pettit, L. *Anal. Chim. Acta* **1967**, *38*, 475–488.

(12) Zékány, L.; Nagypál, I. In *Computational Method for Determination of Formation Constants*; Legett, D. J., Ed.; Plenum: New York, 1985; pp 291–353.

(13) Pagado, J. M.; Goldberg, D. E.; Fernelius, W. C. *J. Phys. Chem.* **1961**, *65*, 1062.

(14) Beck, M. T.; Nagypál, I. In *Chemistry of Complex Equilibria*; Kállay-Tóth, E. K., Ed.; Akadémia Kiadó Budapest and Nostand Reinhold Company Ltd.: London, 1990.

(15) May, P. M.; Williams, D. R.; Linder, P. W. *J. Chem. Soc., Dalton Trans.* **1977**, 588.

(16) Berthon, G.; Hacht, R.; Blais, M.; May, P. M. *Inorg. Chim. Acta* **1986**, *125*, 219.

(17) Cacheris, W. P.; Quay, S. C.; Rocklage, S. M. *Magn. Reson. Imaging* **1990**, *8*, 467.

(18) Jackson, G. E.; Wynchank, S.; Woudenberg, M. *Magn. Reson. Med.* **1990**, *16*, 57.

(19) Baranyai, Z.; Pálinkás, Z.; Uggeri, F.; Brücher, E. *Eur. J. Inorg. Chem.* **2010**, 1948.

(20) Jakab, S.; Kovács, Z.; Burai, L.; Brücher, E. *Magy. Kém. Foly.* **1993**, *99*, 391–396.

(21) Martell, A. E.; Smith, R. M. *Critical Stability Constants*; Plenum Press: New York, 1974: Vol. *4*.
(22) Thompson, M. K.; Botta, M.; Nicolle, G.; Helm, L.; Aime, S.; Merbach, A. E.; Raymond, K. N. *J. Am. Chem. Soc.* **2003**, *125*, 14274.
(23) Banci, L.; Bertini, I.; Luchinat, C. *Nuclear and Electron Relaxation. The Magnetic Nucleus-Unpaired Electron Coupling in Solution*; VCH: Weinheim, Germany, 1991. Bloembergen, N.; Morgan, L. O. *J. Chem. Phys.* **1961**, *34*, 842.
(24) Hwang, L. P.; Freed, J. H. *J. Chem. Phys.* **1975**, *63*, 4017. Freed, J. H. *J. Chem. Phys.* **1978**, *69*, 4034.
(25) Swift, T. J.; Connick, R. E. J. *J. Chem. Phys.* **1962**, *37*, 307−312. Powel, D. H. *J. Am. Chem. Soc.* **1996**, *118*, 9333.
(26) Caravan, P.; Astashkin, A. V.; Raitsimring, A. M. *Inorg. Chem.* **2003**, *42*, 3972.
(27) Botta, M.; Aime, S.; Barge, A.; Bobba, G.; Dickins, R. S.; Parker, D.; Terreno, E. *Chem.—Eur. J.* **2003**, *9*, 2102.
(28) Terreno, E.; Botta, M.; Boniforte, P.; Bracco, C.; Milone, L.; Mondino, D.; Uggeri, F.; Aime, S. *Chem.—Eur. J.* **2005**, *11*, 5531.
(29) Bruce, J. I.; Dickins, R. S.; Govenlock, L. J.; Gunnlaugsson, T.; Lopinski, S.; Lowe, P. M.; Parker, D.; Peacock, R. D.; Perry, J. J. B.; Aime, S.; Botta, M. *J. Am. Chem. Soc.* **2000**, *122*, 9674.
(30) Dickins, R. S.; Aime, S.; Barsanov, A.; Beeby, A.; Botta, M.; Bruce, J. I.; Howard, J. A. K.; Love, C. S.; Parker, D.; Peacock, R. D.; Puschmann, H. *J. Am. Chem. Soc.* **2002**, *124*, 12697.
(31) Moriggi, L.; Canizzo, C.; Prestinari, C.; Barriere, F.; Helm, L. *Inorg. Chem.* **2008**, *47*, 8357.
(32) Burai, L.; Hietapelto, V.; Király, R.; Tóth, E.; Brücher, E. *Magn. Reson. Med.* **1997**, *38*, 146.
(33) (a) Botta, M. *Eur. J. Inorg. Chem.* **2000**, 309. (b) Jacques, V.; Dumas, S.; Sun, W.-C.; Troughton, J. S.; Greenfield, M. T.; Caravan, P. *Invest. Radiol.* **2010**, *45*, 613.